Robertus, J. D., Kraut, J., Alden, R., & Birktoft, J. J. (1972) *Biochemistry 11*, 4293-4303.
Schmid, M. F., Weaver, L. H., Holmes, M. A., Grütter, M. G., Ohlendorf, D. H., Reynolds, R. A., Remington, S. J., & Matthews, B. W. (1981) *Acta Crystallogr. A37*, 701-710.
Schoellmann, G., & Shaw, E. (1963) *Biochemistry 2*, 252-255.
Segal, D. M., Powers, J. C., Cohen, G. H., & Davies, D. R. (1971) *Biochemistry 10*, 3728-3738.
Sigler, P. B., Skinner, H. C. W., Coulter, C. L., Kallos, J., Braxton, H., & Davies, D. R. (1964) *Proc. Natl. Acad. Sci. U.S.A. 51*, 1146-1151.
Tronrud, D. E., Ten Eyck, L. F., & Matthews, B. W. (1987) *Acta Crystallogr. A43*, 489-503.
Tsukada, H., & Blow, D. M. (1985) *J. Mol. Biol. 184*, 703-711.
Yapel, A., Han, M., Lumry, R., Rosenberg, A., & Schiao, D. F. (1966) *J. Am. Chem. Soc. 88*, 2573-2584.

A Nuclear Overhauser Effect Investigation of the Molecular and Electronic Structure of the Heme Crevice in Lactoperoxidase†

V. Thanabal and Gerd N. La Mar*
Department of Chemistry, University of California, Davis, California 95616
Received October 21, 1988; Revised Manuscript Received April 28, 1989

ABSTRACT: The proton homonuclear nuclear Overhauser effect, NOE, in conjunction with paramagnetic-induced dipolar relaxation, is utilized to assign resonances and to probe the molecular and electronic structures of the heme cavity in the low-spin cyanide complex of resting-state bovine lactoperoxidase, LPO-CN. Predominantly primary NOEs were detected in spite of the large molecular weight ($\sim 78 \times 10^3$) of the enzyme, which demonstrates again the advantage of paramagnetism suppressing spin diffusion in large proteins. Both of the nonlabile ring protons of a coordinated histidine are located at resonance positions consistent with a deprotonated imidazole. Several methylene proton pairs are identified, of which the most strongly hyperfine-shifted pair is assigned to the unusual chemically functionalized 8-(mercaptomethylene) group of the prosthetic group [Nichol, A. W., Angel, L. A., Moon, T., & Clezy, P. S. (1987) *Biochem. J. 247*, 147-150]. The large 8-(mercaptomethylene) proton contact shifts relative to that of the only resolved heme methyl signal are rationalized by the additive perturbations on the rhombic asymmetry of the functionalization of the 8-position and the alignment of the axial histidyl imidazole projection along a vector passing through pyrrole A and C of the prosthetic group. Such a stereochemistry is consistent with the resolution of only a single heme methyl group, 3-CH_3, as observed. A pair of hyperfine-shifted methylene protons, as well as a low-field hyperfine-shifted labile proton signal, exhibit dipolar connectivities similar to those previously reported for the distal arginine and histidine, respectively, of horseradish peroxidase [Thanabal, V., de Ropp, J. S., & La Mar, G. N. (1988) *J. Am. Chem. Soc. 110*, 3027-3035], suggesting that these catalytically relevant residues may also exist in LPO.

Heme peroxidases share the common property of reaction with peroxides to yield a pair of reactive intermediates 1 and 2 oxidizing equiv above the high-spin ferric resting state (Dunford & Stillman, 1976; Morrison & Schonbaum, 1979; Dunford, 1982). These oxidizing equivalents are stored on the iron (Fe^{IV}=O for compound II), with the second one residing largely as a cation radical [porphyrin for horseradish peroxidase, HRP,[1] (Dolphin et al., 1971); amino acid side chain in cytochrome *c* peroxidase, C*c*P (Yonetani & Ray, 1965)]. On the basis of the detailed X-ray structural features determined for the various derivatives of C*c*P (Poulos & Kraut, 1980; Finzel et al., 1984; Edwards et al., 1987), it has been proposed that a general feature of the catalytic site of heme peroxidase would include a distal His to act as a base to transfer a proton and a distal Arg to provide stabilization for the heterolytic cleavage of the O-O bond. While similar crystallographic data are not yet available for HRP, partial sequence homology (Welinder, 1979; Takio et al., 1980) and computer modeling (Sakurada et al., 1986) have indicated the presence of these catalytically relevant residues, and detailed solution ^{1}H NMR studies of HRP-CN have unequivocally established not only the presence of both distal His and Arg but with detailed stereochemistry virtually identical with that of C*c*P (Thanabal et al., 1987a,b, 1988a,b).

Lactoperoxidase, LPO, present in mammalian milk, saliva, and tears, is involved in bacterial defense through the oxidation of thiocyanate ion (Hamon & Klebanoff, 1973). The glycoprotein possesses a heme which is extraordinarily tightly bound to a single polypeptide chain with $M_r \sim 78 \times 10^3$ (10% carbohydrate) (Carlstrom, 1969; Sievers, 1981). Originally, partial extraction led to small yields of a porphyrin which appeared to be normal, noncovalently bound protoporphyrin, suggesting that the heme resides in a buried pocket (Sievers, 1979, 1980). More recent work based on reductive cleavage with mercaptoethanol has resulted in a structure for the extracted heme prosthetic group as shown in Figure 1A, where

† This research was supported by a grant from the National Institutes of Health (GM 26226).

[1] Abbreviations: C*c*P, cytochrome *c* peroxidase; HRP, horseradish peroxidase; LPO, lactoperoxidase; NMR, nuclear magnetic resonance; NOE, nuclear Overhauser effect; ppm, parts per million; DSS, 2,2-dimethyl-2-silapentane-5-sulfonate.

0006-2960/89/0428-7038$01.50/0

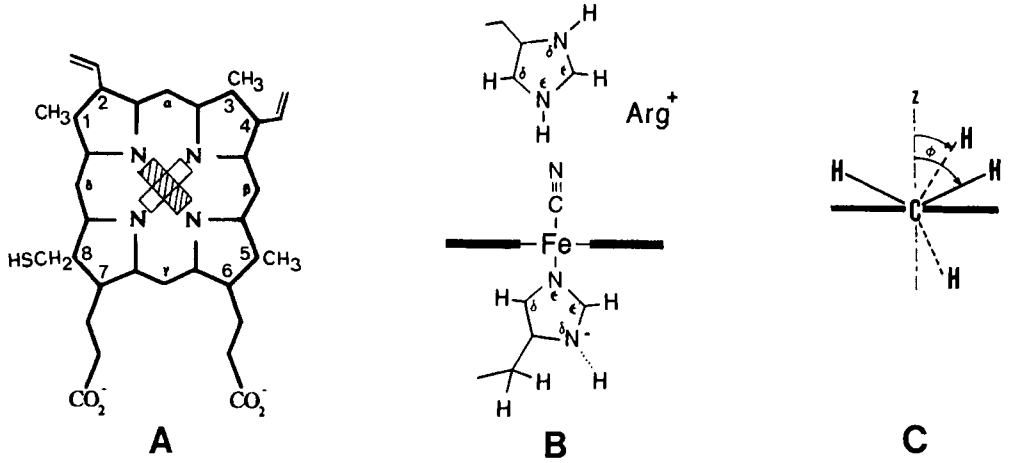

FIGURE 1: (A) Structure and numbering system for the hemin in LPO–CN. The methyl group at the 8-position of the protohemin IX is replaced by a mercapto methylene group (Nichol et al., 1987). The two likely orientations of the proximal histidyl imidazole plane are shown as shaded and open rectangles along the N–Fe–N vectors. The shaded orientation along the pyrroles I and III is consistent with the observed dipolar shifts of the pyrrole substituents (see text). (B) Schematic representation of the proposed active site in LPO–CN. The hemin plane is shown as a horizontal line, and the proximal and the distal histidines are also shown along with their numbering system. The proximity of a possible arginine residue is also indicated in the distal side. (C) Projection of the 8-CH_2 group relative to the heme plane. The view shown is looking directly at the heme edge (the horizontal line) along the 8-CH_2 group. The vertical dashed line is the normal to the heme plane (along the carbon p_z orbital). The protons with solid lines represent the orientation for an usual CH_2 group, while the protons with dotted lines denote a rotated methylene group with respect to the normal. In the latter case, the protons make a dihedral angle of 30° to the normal of the heme plane resulting in an increased contact shift (see text).

the hemin skeleton is modified only by sulfur insertion at the 8-CH_3 (Nichol et al., 1987). Thus, Nichol et al. (1987) proposed that the inability to reversibly remove the heme from lactoperoxidase is due to the formation of a covalent disulfide link with a polypeptide cysteine side chain.

A number of spectroscopic studies have provided evidence that the two vinyls of the prosthetic group are unaltered (Manthey et al., 1986) and that the most probable axial protein ligand is His (Sievers et al., 1983, 1984; Kitagawa et al., 1983; Shiro & Morishima, 1986; Behere et al., 1985), as found in both *Cc*P and HRP. ^{1}H NMR studies have yielded well-resolved spectra for the low-spin ferric cyanide derivative, LPO–CN (Goff et al., 1985; Shiro & Morishima, 1986). However, beside noting that the chemical shifts are unusual for a low-spin ferric hemoprotein and that the protein preparation appears heterogeneous by NMR, few structural details could be discerned.

The major problem, as is generally the case in structural analysis of paramagnetic proteins by NMR (Morrow & Gurd, 1975; La Mar, 1979; Satterlee, 1986), is resonance assignment, which is complicated for LPO by the inability to reconstitute the protein with isotope-labeled or modified hemins (Sievers, 1979; Nichol et al., 1987). We have shown elsewhere not only that the nuclear Overhauser effect, NOE, is of considerable utility in resonance assignments in paramagnetic proteins (Thanabal et al., 1987a,b, 1988a,b) but that the paramagnetism allows successful detection of primary NOEs in much larger proteins than for diamagnetic systems because of the reduced importance of spin diffusion (Kalk & Berendson, 1976).

We report herein on a NOE and relaxation study of LPO–CN that attempts to assign the hyperfine-shifted resonances to individual heme side chains and to establish the likely presence of the proposed essential catalytic residues, His and Arg (Poulos & Kraut, 1980; Finzel et al., 1984), in the distal pocket (Figure 1B). The anomalous NMR properties (Goff et al., 1985; Shiro & Morishima, 1986) which must be reconciled with the prevailing interpretation of the NMR spectral properties of low-spin hemes are as follows: Why is there but a single contact-shifted heme methyl resolved when in other such systems at least two, and often three, methyl peaks are resolved from the diamagnetic envelope? Why are the strongest contact-shifted resonances single proton peaks, and why are these shifts so much larger than those in other hemoproteins in the same oxidation/spin state? The apparent contact shift pattern for heme substituents is interpreted in terms of a combination of electronic perturbations arising from the unusual heme peripheral substitution (Nichol et al., 1987) and the axial interaction with a deprotonated histidine.

Experimental Procedures

Sample Preparation. Lactoperoxidase, LPO, was purchased from Sigma as a lyophilized salt-free powder. The protein was further purified by passage through a Sephadex G-200 column (50 cm × 2 cm) equilibrated with 25 mM phosphate buffer, pH 7.0 (Manthey et al., 1986). The protein was collected as a major single band. The resulting elute was concentrated in an Amicon ultrafiltration cell with a YM 10 membrane to give a $\gtrsim$1.5 mM protein solution. The ^1H_2O solvent was exchanged several times with ^2H_2O containing 25 mM phosphate buffer to give a >99% ^2H_2O sample for NOE measurements. A mixture of 90% ^1H_2O/10% ^2H_2O was used to observe the labile protons resonances. A 42-fold excess of solid KCN was added to generate the cyanide-ligated lactoperoxidase, LPO–CN. The solution pH, adjusted with 0.2 M ^{2}HCl or 0.2 M NaO^{2}H, was measured with a Beckman Model 3550 pH meter equipped with an Ingold microcombination electrode; pH values are not corrected for the isotope effect.

^{1}H NMR Spectra. Nonselective T_1s were determined by a variation of the standard inversion–recovery sequence to include a composite 180° pulse. The ^{1}H NMR spectra with fast pulse repetition rates were recorded with the WEFT or super-WEFT methods (Gupta, 1976). A repetition time as low as 10 ms was used to observe very rapidly relaxing proton resonances. Since large sweep widths (~40 kHz) are necessary to cover the −30 to 80 ppm region, the spectrum was collected with less data points (512) in order to get the recycle time of <10 ms. Consequently, the FID was zero filled three times before Fourier transform to obtain good digital resolution.

The steady-state NOE for an isolated two-spin system is given by (Noggle & Shirmer, 1971)

$$\eta_{i\rightarrow j} = \sigma_{ij}/\rho_j \quad (1)$$

where ρ_j^{-1} is the selective spin–lattice relaxation time of H_j and σ_{ij} is the cross-relaxation between H_i and H_j; $\sigma_{ij} \propto r_{ij}^{-6}\tau$, where r_{ij} is the interproton separation and τ is the molecular tumbling time. For larger proteins ($M_r > 40 \times 10^3$), it is found that an irradiation time of 25–30 ms is close to the steady-state condition without significant spin diffusion (Thanabal et al., 1987a,b, 1988a,b).

Proton NOE measurements were performed on a Nicolet NT-360 FT NMR spectrometer operating at 360 MHz in the quadrature mode. A total of 16 384 data points were collected in double precision over a 40-kHz band width. The NOE experiments were performed according to the pulse sequence $(A[t_1\text{–}t_{on}\text{–P–Acq}]_n\, B[t_1\text{–}t_{off}\text{–P–Acq}]_n)_m$, where A and B designate two different data files, t_1 is a preparation time to allow the relaxation of the resonances (400 ms), t_{on} is the time during which the resonance is kept saturated (25 ms), and t_{off} is an equal time (25 ms) during which the decoupler is set off-resonance. The observed pulse, P, was either a 90° hard pulse (NOEs in ^2H_2O) or a Redfield 2–1–4–1–2 (Redfield et al., 1975) excitation (for H_2O NOE measurements). In the case of Redfield excitation, some attenuation of the transmitter power was applied to obtain a 90° pulse at the carrier; n was set to 96, and the total number of scans in each file ($n \times m$) was (3–4) $\times 10^3$. The NOE difference spectrum was obtained by subtracting B from A.

Primary NOEs are differentiated from off-resonance effects by their independence of the decoupler power or degree of saturation. Off-resonance saturation is approximately inverse quadratically dependent on decoupler power, and NOEs from off-resonance saturated peaks can be easily established by saturating the peak on-resonance (Thanabal et al., 1987a,b, 1988a,b). Each of these controls was executed in the interpretation of each NOE difference spectrum. In the case of closely resonating peaks (peaks x and y in the Figure 4), the off-resonance perturbation was minimized by collecting two spectra with the decoupler frequency on the peak being saturated (on-resonance) and two more spectra with the decoupler frequency being symmetrically off-set by ~500 Hz about the irradiated peak (off-resonance) and then by subtracting the sum of the off-resonance spectra from the sum of the on-resonance spectra. It is noted, however, that significant off-resonance of the diamagnetic envelope is observed in any case (Figure 4). However, the two peaks s and t superimposed on the off-resonance excited envelope exhibit intensities in the difference trace which are independent of the degrees of the off-resonance saturation of the envelope, and hence can be attributed to primary NOEs.

In all of the above ^1H NMR measurements, the signal-to-noise ratio was improved by exponential apodization of the free-induction decay which introduced 20–50-Hz line broadening. Peak shifts were referenced to the residual water signal, which in turn was calibrated against internal 2,2-dimethyl-2-silapentane-5-sulfonate, DSS. Chemical shifts are reported in parts per million, ppm, with downfield shifts taken as positive.

Results

The identification of nonlabile hyperfine-shifted and paramagnetically relaxed resonances in ^2H_2O solution is pursued by utilization of a variety of different pulse repetition rates which discriminate between slowly and rapidly relaxing protons, as illustrated in Figure 2. For slow repetition rates (trace A), we observed signals a–d, x, and y with comparable (one proton; see below) intensities, peak f with three-proton (methyl)

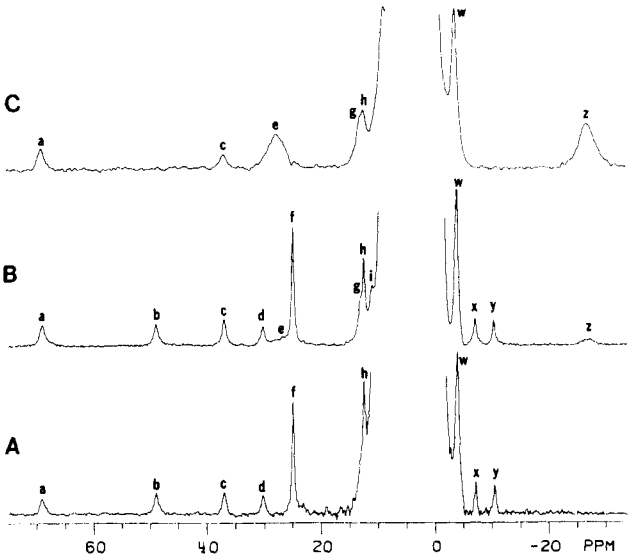

FIGURE 2: 360-MHz ^1H NMR spectrum of 1.5 mM LPO–CN in 99% ^2H_2O at 25 °C, pH 7.0, as a function of the pulse repetition time. (A) Pulse repetition time of 0.5 s^{-1}; this ensures complete relaxation of the hyperfine-shifted peaks. (B) Pulse repetition time of 2 s^{-1} showing reduced intensity for peaks b, d, x, and y. (C) Pulse repetition time of 100 s^{-1} where only the fast-relaxing protons e and z show up with full intensity and most of the other peaks are strongly saturated. In all spectra the resolved peaks are labeled a–i and x–z.

Table I: Chemical Shifts and Proposed Assignments for Heme Cavity Resonances in the Cyanide Complex of Resting-State Lactoperoxidase

peak label	proposed assignment	chemical shift[a]	T_1 (ms)[b]
a	8-CH	68.7	11.6
b	proximal His β-CH (?)	48.7	58
c	8-CH	36.6	17.4
d	(impurity?)	29.9	2×10^2
e	proximal His $C_\delta H$	26.6	<2
f	3-CH_3	24.6	50
g		12.6	
h	distal His $C_\epsilon H$	12.1	
i	proximal His β-CH	10.7	
j	7-$C_\alpha H$ (?)	9.4	
s	distal Arg (?)	0.90	
t	distal Arg (?)	−1.78	
u		−1.37	
v		−1.86	
w	composite	−4.2	
x	distal Arg (?)	−7.4	~10^2
y	distal Arg (?)	−10.7	~10^2
z	proximal His $C_\epsilon H$	−27.5	<2
a*	distal His $N_\epsilon H$	26.0	
b*	distal His $N_\delta H$	16.4	

[a] Shifts in ppm from DSS at 25 °C for sample at pH 7.0. [b] For resolved resonances only in ^2H_2O.

intensity, and composite peaks h (4–5 protons) and w (10–12 protons). The low signal-to-noise is due to the inefficient rate of data collection. Previous reports had identified the same resonances (Goff et al., 1985; Shiro & Morishima, 1986), although reduced intensities suggested peaks b, d, x, and y to originate from a minor protein form. A determination of the nonselective relaxation times for the resolved resonances was carried out under slow pulsing conditions, leading to the T_1 values listed in Table I. It is noted that the relaxation times are typical for a large low-spin ferric hemoprotein (Cutnell et al., 1981; Thanabal et al., 1987a,b, 1988a,b), with the peaks b, d, x, and y exhibiting the longer T_1s; peak d is anomalous in displaying a T_1 unusually long for a strongly shifted proton.

Upon increasing the pulse repetition rate, the signal-to-noise per unit time increases significantly (trace B in Figure 2), revealing the previously reported broad upfield peak z, which

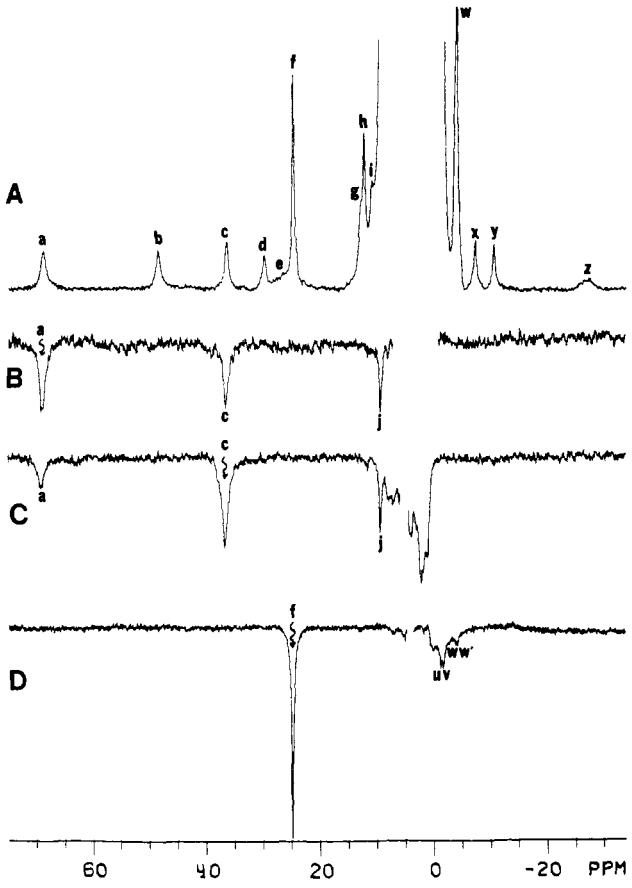

FIGURE 3: 360-MHz ^1H NMR spectrum of (A) 1.5 mM LPO–CN in 99.8% ^2H_2O at 25 °C, pH 7.0, collected at a pulse repetition rate of 2 s^{-1}. The peaks are labeled as in Figure 2. Traces B–D are the NOE difference spectra generated by subtracting the reference spectrum with the decoupler off-resonance from a similar spectrum of the same sample in which the desired resonance was saturated. In each of the traces B–D a downward arrow indicates the peak being saturated. (B) Saturation of peak a shows a strong (~50%) NOE to peak c and a smaller (~20%) NOE to a nonresolved peak designated j. (C) Saturation of peak c; note the strong reciprocal NOE to peak a and a smaller NOE to peak j. The proximity of the decoupler causes weak off-resonance of the diamagnetic envelope. (D) Saturation of peak f; only weak NOEs to peaks u and v and peaks w′ and w″ under the composite peak w, together with very weak off-resonance excitation of the diamagnetic envelope are observed.

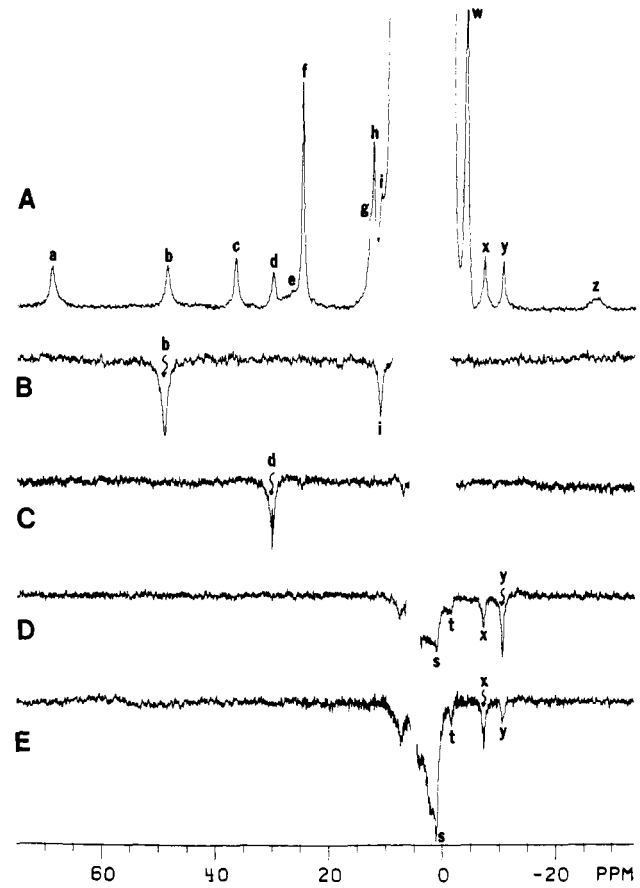

FIGURE 4: 360-MHz ^1H NMR spectrum of (A) 1.5 mM LPO–CN in 99.8% ^2H_2O at 25 °C, pH 7.0, collected with a pulse repetition rate of 2 s^{-1}. The peaks are labeled as in the trace A of Figure 2. Traces B–E are the NOE difference spectra generated as described in Figure 3. In each of the traces B–E, a downward arrow indicates the peak being saturated. (B) Saturation of peak b shows a strong (40%) NOE to partially resolved peak i. (C) Saturation of peak d; note the absence of NOEs to any of the resolved peaks. Saturation of peaks x and y; traces D and E are effected as described under Experimental Procedures. (D) Saturation of peak y; note a strong NOE to peak x and also likely smaller NOEs to peaks s and t superimposed on the off-resonance excited envelope. (E) Saturation of peak x; note the reciprocal NOE to peak y and also smaller NOEs to peaks s and t, again superimposed on the necessarily stronger off-resonance saturation of the diamagnetic envelope.

we determine to have one-proton intensity; a suggestion of a second such broad peak, peak e, is observed in the low-field region between peaks d and f. The intensities of the slowly relaxing protons, b, d, x, and y, are suppressed, as is the intensity of the diamagnetic envelope, which reveals two additional resonances, g and i with indeterminate intensity although g is likely a single proton. The extremely rapid relaxation rates of peaks z and e are emphasized in the super-WEFT trace (C) of Figure 2, for which only e and z have completely relaxed and exhibit the same (single proton) intensity. The importance of the differential T_1s and pulse repetition rates on the relative intensities of the various resonances is noted.

The results of NOE studies are presented in Figures 3–5. In each case, the saturation of a hyperfine-shifted resonance had two effects. Clear evidence for primary NOEs was obtained where the intensity of a discernible peak (whether resolved or in the diamagnetic envelope) in the NOE difference traces was linear in the degree of saturation of the irradiated peak (Thanabal et al., 1987a,b, 1988a). However, the large decoupler power needed to effectively saturate resonances, together with the extremely large intensity of the diamagnetic protein envelope (containing ~4×10^3 protons), always leads to off-resonance saturation of the diamagnetic envelope and residual solvent line even when the reference spectrum has the decoupler symmetric to the envelope (Thanabal, 1987b). This effect is particularly acute when peaks close to the diamagnetic envelopes are saturated. The off-resonance effect, however, can be identified by noting the very dramatic drop with decoupler power and the fact that it is similarly observed when the decoupler is placed near a peak rather than precisely on-resonance.

Saturating peak a yields a large (~50%) NOE to peak c and a smaller (~20%) NOE to an unresolved peak we label j (spectrum B in Figure 3). The reciprocal NOE to peak a (~25%) is observed when saturating peak c (spectrum C in Figure 3), as well as a smaller NOE (10–15%) to the same peak j. The irradiation of methyl peak f yields small NOEs to upfield unresolved peaks u and v and to two peaks, w′ and w″, with shifts indicating that they are components of the composite peak w (Figure 3D). The saturation of peak b leads primarily to a large (~40%) NOE to a peak (spectrum B in Figure 4) with chemical shift identical with that of the partially resolved peak i identified in spectrum B of Figure 2. The line width of peak i, together with its intensity in the reference spectrum, argues for peak i arising from a single proton. Irradiation of peak d exhibits only small apparent NOEs to

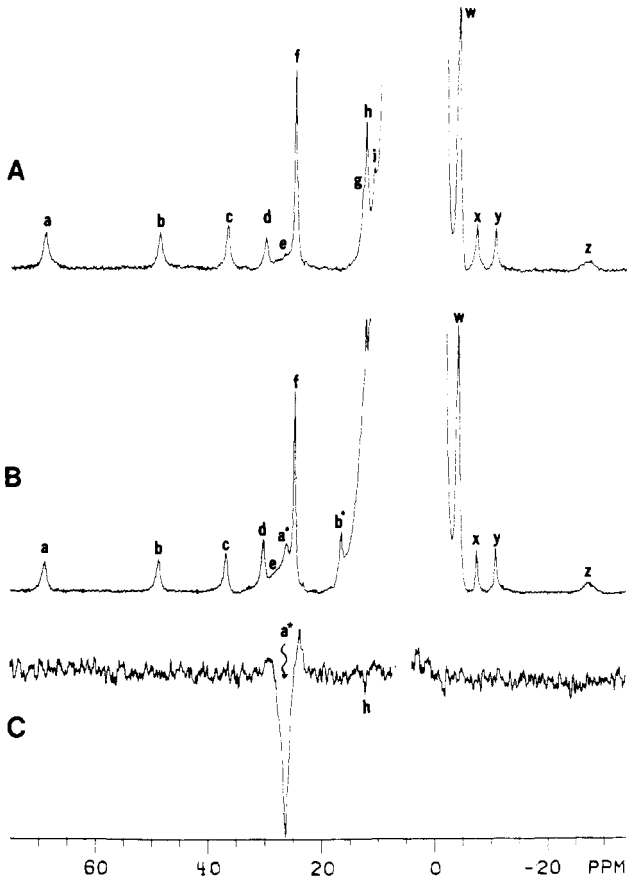

FIGURE 5: 360-MHz ^1H NMR spectrum of 1.5 mM LPO–CN in 99.8% ^2H_2O (A) and in 90% H_2O/10% ^2H_2O (B) at 25 °C, pH 7.0, with pulse repetition rate of 2 s^{-1}. The spectrum in 90% H_2O/10% ^2H_2O was collected with the use of a Redfield 2–1–4–1–2 pulse sequence optimized for the window 10–70 ppm. The resolved nonlabile proton peaks in both the spectra are labeled as in Figure 2. Trace B shows two additional peaks, a* and b*, that arise from labile protons. Trace C shows the NOE difference spectrum upon saturation of peak a*; note a NOE to peak h or a component of peak h. Saturation of peak a* is also performed as described for peaks x and y in Figure 4.

an unresolved resonance (spectrum C in Figure 4). Saturation of the upfield peaks x and y always caused large off-resonance effects because of the proximity of these peaks to the envelope. However, saturating peak y (spectrum D of Figure 4) yields an obvious large (~50%) NOE to peak x (which is linear in the degree of saturation of peak y, and hence definitely not an off-resonance effect). Moreover, superimposed on the off-resonance excited diamagnetic envelope, we note additional likely NOEs to peaks labeled s and t. The NOEs to peaks s and t are also (and more clearly) observed when peak x is saturated (spectrum E of Figure 4), which also yields a reciprocal large NOE to peak y. The broad and fast-relaxing resonances e and z could not be saturated sufficiently to allow detection of any NOEs.

The traces of LPO–CN in ^2H_2O and ^1H_2O are compared in spectra A and B of Figure 5 and clearly identify exchangeable proton resonances a* (broad like peak a) and b* (narrow, like peaks x and y) at 26.0 and 16.45 ppm, respectively; the former peak had been previously reported and proposed to arise from the proximal His ring proton (Shiro & Morishima, 1986). Peak a* could be effectively saturated and leads to an NOE to a very narrow peak (~50 Hz) which is not clearly resolved (spectrum C in Figure 5) but whose shift is coincident with that of composite peak h in spectrum B of Figure 2. The labile proton peak b* is on the edge of both the envelope and the intense solvent resonance and could not be effectively saturated without inducing strong artifacts in the region 0–10 ppm.

Discussion

Protein Heterogeneity. It has been suggested that peaks b, d, x, and y exhibit less than one-proton intensity in various LPO preparations and that peak z may contain more than one proton. In our preparations, we note that all five of these peaks exhibit single-proton intensity *when observed under nonsaturating conditions.* It is particularly noted that rapid pulsing tends to decrease the intensity primarily for peak d ($T_1 \sim 200$ ms) and next for peaks b, x, and y (which have the next longest T_1s). NOE connectivities discussed below argue for at least peaks b, x, and y arising from the major protein component.

Identification of Functional Groups. The large (~50%) NOEs observed between peaks a and c, and peaks x and y argue strongly for their origin in two pairs of geminal methylene protons. Similarly large NOEs have been observed for pairs of single protons in paramagnetic derivatives of both HRP (M_r 42 × 10^3) (Thanabal et al., 1987a,b, 1988a,b) and hemoglobin (M_r ~65 × 10^3) (M. J. Chatfield and G. N. La Mar, unpublished observation), where the identity of the pairs of protons as arising from a methylene group could be independently established. The large NOE from peak b to peak i also argues that peak i must be a single proton, and hence peaks b and i represent a third methylene group. The intensity of peak f is consistent with it arising from a heme methyl, as observed in every other low-spin hemoprotein (Morrow & Gurd, 1975; La Mar, 1979; Satterlee, 1986). The likely origin of peaks *x* and *y* as arising from the major component has support from two observations. Under nonsaturating conditions, they exhibit the correct intensities expected for their likely methylene origin. Second, if they arise from a second component, this component would exhibit solely a hyperfine-shifted methylene group which is unprecedented for a heme protein. The reduced intensities reported previously may have arisen due to partial saturation of these slow-relaxing peaks (as well as peak b).

Proximal Histidine Resonances. The upfield broad single-proton peak z had been previously attributed (Shiro & Morishima, 1986) to the axial His nonlabile C_ϵ–H (Figure 1B) on the basis of similar observations in HRP–CN (La Mar et al., 1982), where its assignment could be definitely established by NOEs (Thanabal et al., 1987b). The detection of the second, similarly relaxed, broad resonance e, again at essentially the same position as in HRP–CN (with similar relaxation times), provides strong support for the assignment of both peaks e and z to the proximal His C_δ–H and C_ϵ–H and a bound His environment very similar to that of HRP–CN, i.e., a deprotonated imidazolate (Thanabal et al., 1987b, 1988a). The imidazolate character of the proximal His argues against the previous assignment of labile proton a* to N_δH (Shiro & Morishima, 1986).

The axial His β-CH_2 signals are observed in HRP–CN and C*c*P–CN with mean shifts of ~15 ppm and exhibit ~50% NOEs between them (Thanabal et al., 1987b). Even smaller β-CH_2 shifts are found in the appropriate imidazolate model compound (Chacko & La Mar, 1982). The very similar axial imidazolate ring shifts for peaks e and z as the same assigned peaks in HRP–CN (Thanabal et al., 1987b) make significant changes in this mean β-CH_2 shift extremely unlikely. Hence, peaks b and i could arise from the His β-CH_2, while the large mean shift of ~50 ppm makes the peaks a and c CH_2 group a very unlikely candidate.

Heme Resonances. A distinctive feature of low-spin ferric heme proteins is that a combination of the asymmetric pe-

ripheral substituents and protein-based contacts exerts a strong rhombic perturbation on the heme electronic structure which can be correlated primarily with the orientation of the projection of the axial His imidazole plane relative to individual pyrroles (Shulman et al., 1971; Traylor & Berzinis, 1980; La Mar, 1979; Satterlee, 1986). This results in large contact shifts for the substituents on opposite pyrroles, i.e., pyrroles I and III or pyrroles II and IV, depending on whether the axial imidazole orientation is as depicted by the open or shaded rectangle in A of Figure 1. The former axial His imidazole orientation would predict large low-field contact shifts for two methyls (1-CH_3 and 5-CH_3) (as well as possibly 4-H_α shifts), as observed in metcyano complexes of Mb (Mayer et al., 1974) and HbA (La Mar et al., 1988), while the latter orientation would predict large low-field contact shifts for one methyl group [3-CH_3; as found in cytochrome *c* peroxidase (Satterlee et al., 1983)] and possibly the anomalous 8-SCH_2 group and the 4-vinyl H_α. The observation of only a single low-field methyl for LPO–CN thus favors the latter orientation, with peak f due to 3-CH_3. The large contact shift for the methylene group giving rise to peaks a and c would thus arise either from the unusual 8-SCH_2 group or from the adjacent 7α-CH_2.

The unprecedented large contact shifts for peaks a and c support their origin as 8-SCH_2 rather than 7α-CH_2 for the following reason. The heme α-methylene protons experience contact shifts, δ_{con}, related to the adjacent pyrrole carbon π spin density, ρ_π, via (La Mar, 1973)

$$\delta_{con} = \rho_\pi B \cos^2 \phi \qquad (2)$$

where ϕs is the dihedral angle between the C–C–H plane and the aromatic carbon p_z axis (Figure 1C) and B is a constant. In a rotating methyl group, $\langle \cos^2 \phi \rangle = 0.50$. In a usual methylene group, as found for hemin propionate or ethyl groups, $\phi \sim 60$ (Figure 1C, dark lines), leading to $\cos^2 \phi \sim 0.25$ and accounting for the much smaller α-CH_2 relative to CH_3 contact shifts observed in low-spin ferric hemes [La Mar & Walker (Jensen), 1978]. The covalent link to the protein, however, could lead to a 8-SCH_2 orientation as in Figure 1C (dotted lines) for which $\phi \sim 30°$ and $\cos^2 \phi = 0.75$, *leading to ~50% larger contact shifts for an α-CH_2* than a CH_3 group for the same π spin density and a 3 times larger shift than that for the usual unconstrained orientation of an α-CH_2 group. This effect can therefore account for the large contact shifts for the methylene protons a and c. Thus, the assignment of peak f to 3-CH_3 and peaks a and c to 8-SCH_2 is consistent with both the unusual heme contact shift pattern and the previously proposed functionalization of the 8-methyl group via a constrained disulfide link to the protein matrix. Other NMR spectral features are less distinct. The NOE for peaks a and c to peak j suggests peak j arises from an adjacent 7α-CH. The small upfield NOEs to peaks labeled u, v, w′, and w″ upon saturating peak f, the likely 3-CH_3, suggest two of these could arise from the 4-vinyl H_βs.

Noncoordinated Amino Acids. The upfield apparent methylene group that gives rise to peaks x and y is also close to another pair of protons, s and t. A potential origin for peaks x and y and for peaks s and t could be the two methylene groups of a heme propionate. However, at least the α-CH_2 shifts of a propionate are generally downfield [La Mar & Walker (Jensen), 1978]. An alternate interpretation is that they arise from an amino acid with at least a CH_2–CH_2 chain. We note that the orientation of the axial His imidazole plane deduced above is the same as that found in HRP and C*c*P, leading to the expectation that the dipolar shifts are similar in these three systems (Thanabal et al., 1987a,b, 1988a,b). HRP–CN exhibited two sets of upfield-coupled CH_2 signals which could be demonstrated to arise from Arg 38 in contact with pyrrole III (Thanabal et al., 1987b). The upfield dipolar shifts of peaks x, y, s, and t suggest the possibility that these signals arise from a similarly situated amino acid, and the dipolar connectivities are consistent with, but not proof for, an Arg residue. The slower relaxation of peaks x and y relative to that of the heme methyl peak f would argue that this residue is further from the iron in LPO than in HRP.

Two hyperfine-shifted labile proton signals are resolved, a* (broad, ~200 Hz) and b* (narrow, 80 Hz) at 26 and 16.4 ppm, respectively, which must arise from one or more amino acids. HRP–CN exhibits two labile proton signals with very similar hyperfine shifts and relative line width, and we demonstrated that both arise from the ring of the distal His 42 by observing NOEs from both labile protons to the mutually neighboring $C_\epsilon H$ (Thanabal et al., 1988a,b). In the present case of LPO–CN, no narrow nonlabile proton is resolved from the diamagnetic envelope. However, as in the case for HRP–CN (Thanabal et al., 1988a,b), saturating peak a* leads to a NOE for a narrow peak (~60 Hz) on the edge of the intense diamagnetic envelope (Figure 5C), supporting the assignment of peak a* and a component of peak h to the $N_\epsilon H$ and $C_\epsilon H$, respectively, of a distal His with stereochemistry similar to that found for the distal His in C*c*P (Poulos & Kraut, 1980) and HRP (Figure 1B) (Thanabal et al., 1987b, 1988a,b). The second labile proton (b*) resonates on the shoulder of the diamagnetic envelope and intense ^1H_2O signal, as well as close to peak h, and does not allow us to establish its identity using NOEs. However, its shift and line-width similarity to those in HRP–CN suggest peak b* arises from the other ring labile proton ($N_\delta H$) of a protonated distal His (Thanabal et al., 1988a).

Conclusions

The nuclear Overhauser effect provides a valuable tool for resonance assignment and the investigataon of the molecular structure of large paramagnetic proteins. This is the largest protein for which successful NOE studies have been reported. Clearly primary NOEs as observed in all cases indicate that spin diffusion to the diamagnetic matrix is significantly reduced as compared to the expectations for an analogous diamagnetic protein.

The proposed assignments based on NOE connectivities yield a contact shift pattern that is consistent with the structure of the derivatized heme as shown in Figure 1A, with an axial imidazolate plane oriented primarily along the N–Fe–N axis of pyrroles I and III, as shown by the shaded rectangle in Figure 1A. The upfield-shifted nonlabile narrow signals and low-field-shifted labile proton signals are shown to have NOE connectivities consistent with, but not proof for, a distal Arg and His with stereocehmistry in the distal pocket qualitatively similar to that in C*c*P and HRP.

Registry No. Heme, 14875-96-8.

References

Behere, D. V., Gonzalvez-Vergara, E., & Goff, H. M. (1985) *Biochim. Biophys. Acta 32*, 319–325.

Carlstrom, A. (1969) *Acta Chem. Scand. 23*, 185–213.

Chacko, V. P., & La Mar, G. N. (1982) *J. Am. Chem. Soc. 104*, 7002–7007.

Cutnell, J. D., La Mar, G. N., & Kong, S. B. (1981) *J. Am. Chem. Soc. 103*, 3567–3572.

Dolphin, D., Forman, A., Borg, D. C., Fajer, J., & Felton, R. H. (1971) *Proc. Natl. Acad. Sci. U.S.A. 68*, 614–618.

Dunford, H. B. (1982) *Adv. Inorg. Biochem. 4*, 41–68.

Dunford, H. B., & Stillman, J. S. (1976) *Coord. Chem. Rev. 19*, 187–251.
Edwards, S. L., Xuong, Ng. H., Hamlin, R. C., & Kraut, J. (1987) *Biochemistry 26*, 1503–1511.
Finzel, B. C., Poulos, T. L., & Kraut, J. (1984) *J. Biol. Chem. 259*, 13027–13036.
Goff, H. M., Gonzalvez-Vergara, E., & Ales, D. C. (1985) *Biochem. Biophys. Res. Commun. 133*, 794–799.
Gupta, R. K. (1976) *J. Magn. Reson. 24*, 461–465.
Hamon, C. B., & Klebanoff, S. I. (1973) *J. Exp. Med. 137*, 438–450.
Kalk, A., & Berendsen, J. J. C. (1976) *J. Magn. Reson. 24*, 343–366.
Kitagawa, T., Hashimoto, S., Teroaka, J., Nakamura, S., Yajima, H., & Hosoya, T. (1983) *Biochemistry 22*, 2788–2792.
La Mar, G. N. (1973) in *NMR of Paramagnetic Molecules* (La Mar, G. N., Horrocks, W. D., Jr., & Holm, R. H., Eds.) pp 85–126, Academic, New York.
La Mar, G. N. (1979) in *Biological Applications of Magnetic Resonance* (Shulman, R. G., Ed.) pp 305–343, Academic, New York.
La Mar, G. N., & Walker (Jensen), F. A. (1978) in *The Porphyrins* (Dolphin, D., Ed.) Vol. IVB, pp 61–157, Academic Press, New York.
La Mar, G. N., Viscio, D. B., Smith, K. M. Caughey, W. S., & Smith, M. L. (1978a) *J. Am. Chem. Soc. 100*, 8085–8092.
La Mar, G. N., Viscio, D. B., Gersonde, K., & Sick, H. (1978b) *Biochemistry 17*, 361–367.
La Mar, G. N., de Ropp, J. S., Chacko, V. P., Satterlee, J. D., & Erman, J. E. (1982) *Biochim. Biophys. Acta 708*, 317–325.
La Mar, G. N., Jue, T., Nagai, K., Smith, K. M., Yamamoto, Y., Kauten, R. J., Thanabal, V., Langry, K. C., Pandey, R. K., & Leung, H.-K. (1988) *Biochim. Biophys. Acta 952*, 131–144.
Manthey, J. A., Boldt, N. J., Bocian, D. F., & Chan, S. I. (1986) *J. Biol. Chem. 261*, 6734–6741.
Mayer, A., Ogawa, S., Shulman, R. G., Yamane, T., Cavalevio, J. A. S., Rocha-Gonsalves, A. M. d'A., Kenner, G. W., & Smith, K. M. (1974) *J. Mol. Biol. 86*, 749–756.
Morrison, M., & Schonbaum, G. R. (1979) *Annu. Rev. Biochem. 45*, 861–888.
Morrow, J. S., & Gurd, F. R. N. (1975) *CRC Crit. Rev. Biochem. 3*, 221–287.
Nichol, A. W., Angel, L. A., Moon, T., & Clezy, P. S. (1987) *Biochem. J. 247*, 147–150.
Noggle, J. H., & Shirmer, R. E. (1971) *The Nuclear Overhauser Effect*, Academic, New York.
Poulos, T. L., & Kraut, J. (1980) *J. Biol. Chem. 255*, 8199–8205.
Redfield, A. G., Kunz, S. D., & Ralph, E. K. (1975) *J. Magn. Reson. 19*, 114–117.
Sakurada, J., Takahashi, S., & Hosoya, T. (1986) *J. Biol. Chem. 261*, 9657–9662.
Satterlee, J. D. (1986) *Annu. Rep. NMR Spectrosc. 17*, 79–178.
Satterlee, J. D., Erman, J. E., La Mar, G. N., Smith, K. M., & Langry, K. C. (1983) *J. Am. Chem. Soc. 105*, 2099–2104.
Shiro, Y., & Morishima, I. (1986) *Biochemistry 25*, 5844–5849.
Shulman, R. G., Glarum, S. H., & Karplus, M. (1971) *J. Mol. Biol. 57*, 93–115.
Sievers, G. (1979) *Biochim. Biophys. Acta 579*, 180–190.
Sievers, G. (1980) *Biochim. Biophys. Acta 624*, 249–259.
Sievers, G. (1981) *FEBS Lett. 127*, 253–256.
Sievers, G., Gadsby, P. M. A., Peterson, J., & Thomson, A. J. (1983) *Biochim. Biophys. Acta 742*, 659–668.
Sievers, G., Peterson, J., Gadsby, P. M. A., & Thomson, A. J. (1984) *Biochim. Biophys. Acta 785*, 7–13.
Takio, K., Titani, K., Ericsson, L. H., & Yonetani, T. (1980) *Arch. Biochem. Biophys. 203*, 615–629.
Thanabal, V., de Ropp, J. S., & La Mar, G. N. (1986) *J. Am. Chem. Soc. 108* 4244–4245.
Thanabal, V., de Ropp, J. S., & La Mar, G. N. (1987a) *J. Am. Chem. Soc. 109*, 265–272.
Thanabal, V., de Ropp, J. S., & La Mar, G. N. (1987b) *J. Am. Chem. Soc. 109*, 7516–7525.
Thanabal, V., de Ropp, J. S., & La Mar, G. N. (1988a) *J. Am. Chem. Soc. 110*, 3027–3035.
Thanabal, V., La Mar, G. N., & de Ropp, J. S. (1988b) *Biochemistry 27*, 5400–5407.
Traylor, T. G., & Berzinis, A. P. (1980) *J. Am. Chem. Soc. 102*, 2844–2846.
Unger, S. W., Jue, T., & La Mar, G. N. (1985) *J. Magn. Reson. 61*, 448–456.
Welinder, K. G. (1979) *Eur. J. Biochem. 96*, 483–502.
Yonetani, T., & Ray, G. S. (1965) *J. Biol. Chem. 240*, 4503–4508.